

# Doubly-Robust Functional Average Treatment Effect Estimation

**Lorenzo Testa**

*Department of Statistics & Data Science, Carnegie Mellon University  
L'EMbeDS, Sant'Anna School of Advanced Studies*

LORENZO@STAT.CMU.EDU

**Tobia Boschi**

*IBM Research Europe*

TOBIA.BOSCHI@IBM.COM

**Francesca Chiaromonte**

*Department of Statistics, Penn State University  
L'EMbeDS, Sant'Anna School of Advanced Studies*

FXC11@PSU.EDU

**Edward H. Kennedy**

*Department of Statistics & Data Science, Carnegie Mellon University*

EDWARD@STAT.CMU.EDU

**Matthew Reimherr\***

*Department of Statistics, Penn State University  
Amazon Science*

MLR36@PSU.EDU

## Abstract

Understanding causal relationships in the presence of complex, structured data remains a central challenge in modern statistics and science in general. While traditional causal inference methods are well-suited for scalar outcomes, many scientific applications demand tools capable of handling functional data – outcomes observed as functions over continuous domains such as time or space. Motivated by this need, we propose **DR-FoS**, a novel method for estimating the Functional Average Treatment Effect (FATE) in observational studies with functional outcomes. **DR-FoS** exhibits double robustness properties, ensuring consistent estimation of FATE even if either the outcome or the treatment assignment model is misspecified. By leveraging recent advances in functional data analysis and causal inference, we establish the asymptotic properties of the estimator, proving its convergence to a Gaussian process. This guarantees valid inference with simultaneous confidence bands across the entire functional domain. Through extensive simulations, we show that **DR-FoS** achieves robust performance under a wide range of model specifications. Finally, we illustrate the utility of **DR-FoS** in a real-world application, analyzing functional outcomes to uncover meaningful causal insights in the SHARE (*Survey of Health, Aging and Retirement in Europe*) dataset.

**Keywords:** functional data analysis, causal inference, semiparametric statistics, missing data, double robustness

## 1 Introduction

Causal inference has become a foundational tool for understanding the effects of interventions in a variety of fields, including medicine (Prosperi et al., 2020), economics (Varian, 2016), and the social sciences (Imbens, 2024). Most causal inference methods are developed for settings in which the outcome of interest is a scalar variable, such as a single measurement of health status or income level. However, there is a growing need to expand

\*Work does not relate to the author's position at Amazon.

these methods to accommodate more complex data structures, particularly functional data, where the outcome is observed as a function over a continuous domain, such as time or space (Kokoszka and Reimherr, 2017; Ramsay and Silverman, 2005). Functional outcomes arise in numerous applications, such as longitudinal studies where medical or wearable devices are used to record patients’ biometrics over time (Boschi et al., 2024a; Jeong et al., 2024; Lundborg et al., 2022), epidemiological studies where infectious diseases are tracked across spatiotemporal domains (Boschi et al., 2021, 2023), and neuroscience studies where brain activity is monitored over time and space (Boschi et al., 2024c; Qi and Luo, 2018). Functional data introduces specific challenges to causal inference, necessitating theory and methodology that can capture the infinite-dimensional nature of these outcomes while providing reliable estimates of treatment effects.

Despite the scientific relevance of this problem, the estimation of treatment effects in functional data settings has not received much attention. The primary challenge lies in handling the complexity of functional data, which requires specialized tools to account for the structure and dependencies across the continuous domain. Traditional scalar methods for estimating treatment effects cannot be applied directly, and current functional data techniques either are designed for settings without access to additional covariates (Cremona et al., 2018) or model outcomes with non-robust tools such as function-on-scalar regression (Ecker et al., 2024; Ieva et al., 2025), which may perform poorly if the model is misspecified. A relevant exception is Liu et al. (2024) – where the authors provide, under strong parametric assumptions, an estimator that can be robust to some forms of model misspecification.

In this paper, we introduce the Doubly-Robust Function-on-Scalar estimator (**DR-FoS**), a novel approach for estimating the Functional Average Treatment Effect (FATE) in settings with functional outcomes. Our proposed method draws from the concept of double robustness, a property in causal inference that provides consistent estimation even if only one of two models – either the outcome model or the treatment assignment model – is correctly specified. Double robustness has been widely used in scalar treatment effect estimation, particularly through methods such as Augmented Inverse Probability Weighting (AIPW) and Targeted Maximum Likelihood Estimation (Tsiatis, 2006; Van Der Laan and Rubin, 2006). The extension of double robustness to functional data requires a careful analysis of the underlying functional structure and the choice of estimation strategies that can handle high-dimensional functional representations. **DR-FoS** leverages recent advances in functional data analysis, combining ideas from functional central limit theorems (Dette et al., 2020) and simultaneous confidence bands (Liebl and Reimherr, 2023; Pini and Vantini, 2017) with doubly-robust estimation techniques to provide a flexible, theoretically sound estimator for FATE.

The contributions of this paper, building upon prior work in causal inference (Kennedy et al., 2019; Lin et al., 2023) and functional data analysis (Dette et al., 2020), are three-fold. First, we develop the **DR-FoS** estimator, which integrates information from both the outcome model and the treatment assignment model, and features double robustness properties to mitigate the risk of misspecification in either. Second, we rigorously analyze the asymptotic properties of the **DR-FoS** estimator, showing that it converges to a Gaussian process under weak regularity conditions. We also provide, under minimal assumptions, estimation procedures that facilitate the construction of confidence bands with simultaneous

guarantees, thus enabling inference on the estimated functional treatment effects. Finally, as intermediate steps in our proofs, we establish novel results on the asymptotic distribution of the AIPW estimator for the average treatment effect (ATE) in the case of multivariate vector outcomes, and on asymptotic properties of the inverse probability weighting (IPW) estimator for functional outcomes.

To validate the effectiveness of DR-FoS, we conduct a series of simulations that demonstrate its robustness and accuracy under various model misspecification scenarios. Our simulations illustrate that DR-FoS consistently outperforms methods based solely on the estimation of propensity score or outcome regression models, especially under misspecification, underscoring the practical utility of double robustness in functional data settings. Finally, we apply DR-FoS to the SHARE dataset (*Survey of Health, Aging and Retirement in Europe*; Alcser et al. (2005)) analyzing the causal effect of chronic conditions on functional indicators of quality of life.

The remainder of this paper is organized as follows. Section 2 defines the target and gives causal assumptions under which the target is identifiable. Section 3 introduces the estimation procedure and the supporting theoretical results required for inference. Section 4 describes our simulation study, which provides further support for our approach. We then apply DR-FoS to the SHARE dataset in Section 5. Finally, Section 6 contains some concluding remarks. All code for reproducing our analysis is available at <https://github.com/testalorenzo/DR-FoS>.

## 1.1 Notation and setup

Let  $\mathcal{T} = [t_1, t_2]$  be a closed bounded interval. Without loss of generality, one can consider  $\mathcal{T} = [0, 1]$ . We observe a collection of  $n$  independent and identically distributed samples,  $\{\mathcal{D}_i = (A_i, X_i, \mathcal{Y}_i)\}_{i=1}^n$ , where  $A_i \in \{0, 1\}$  is a binary variable that indicates whether subject  $i$  belongs to the treated group ( $A_i = 1$ ) or to the control group ( $A_i = 0$ );  $X_i \in \mathbb{R}^p$  is a  $p$ -dimensional vector of covariates; and  $\mathcal{Y}_i \in C(\mathcal{T})$  is a continuous function representing the outcome defined over  $\mathcal{T}$ . We assume  $C(\mathcal{T})$ , the space of continuous functions over  $\mathcal{T}$ , is equipped with the uniform topology, which induces the sup-norm defined by  $\|f\| = \sup_{t \in \mathcal{T}} |f(t)|$ , for  $f \in C(\mathcal{T})$ , thus making  $(C(\mathcal{T}), \|\cdot\|)$  a Banach space. We denote *weak convergence* of a random object  $W_n$  (which can be either finite or infinite dimensional) to a limit  $W$  as  $W_n \rightsquigarrow W$ . Similarly, we denote *convergence in  $\mathbb{L}^2$  norm* as  $W_n \xrightarrow{\mathbb{L}^2} W$ . Finally, throughout this paper, we let  $\mathcal{D} = (A, X, \mathcal{Y})$  denote an independent copy of  $\mathcal{D}_i = (A_i, X_i, \mathcal{Y}_i)$ .

We would like to stress that our choice of the sup-norm, following Dette et al. (2020), significantly differentiates our work from most of the standard literature on functional data (Bosq, 2000; Ferraty, 2006; Kokoszka and Reimherr, 2017; Ramsay and Silverman, 2005) and causal inference (Liu et al., 2024; Luedtke and Chung, 2024), which instead simplifies the analysis by assuming that functional outcomes exist in a Hilbert space (e.g., the space of square integrable functions  $\mathbb{L}^2$ ). In a Banach space, standard asymptotics breaks down without further assumptions; we thus need to introduce tailored assumptions to be able to prove central limit theorems in this setting. Even more importantly, the inferential problem of constructing confidence bands would be ill-posed in the  $\mathbb{L}^2$  space. In fact, the  $\mathbb{L}^2$  norm provides a measure of the global, average deviation of a function along its

domain, but does not account for pointwise or localized deviations, which are essential for constructing simultaneous confidence bands. Instead, confidence bands require control over the supremum norm, making  $C(\mathcal{T})$ , the space of continuous functions endowed with the sup-norm, the most natural choice for this purpose.

## 2 Definition and identification

Our target is the *functional average treatment effect* (FATE), defined as

$$\beta = \mathbb{E} \left[ \mathcal{Y}^{(1)} - \mathcal{Y}^{(0)} \right], \quad (1)$$

where the expectation is taken over the data generating process. Recall  $\mathcal{Y}$  is a function, so  $\beta$  is as well; we omit function arguments for notational simplicity. In terms of functional analysis, if  $\mathcal{P}$  is the class of probability measures on  $C(\mathcal{T})$ , we can represent our target as a functional  $\psi : \mathcal{P} \rightarrow C(\mathcal{T})$  such that  $\psi(\mathbb{P}) = \beta$ .

Despite the increased complexity of the outcome variable and target, conditions under which the latter is identifiable are standard. In particular, we leverage the following setup.

**Assumption 1 (Identifiability)** *Let the following identifiability assumptions hold:*

- a. Consistency.** *The potential outcome of a treatment is the same regardless of the mechanism by which the treatment is administered; that is,  $\mathcal{Y} = \mathcal{Y}^{(a)}$  if  $A = a$ . Equivalently,  $\mathcal{Y} = A\mathcal{Y}^{(1)} + (1 - A)\mathcal{Y}^{(0)}$ .*
- b. No unmeasured confounding.**  $(\mathcal{Y}^{(0)}, \mathcal{Y}^{(1)}) \perp\!\!\!\perp A \mid X$ .
- c. Positivity.**  $0 < \mathbb{P}[A = 1 \mid X] < 1$  almost surely.

With these assumptions in place, we are ready to introduce the proposed estimator.

## 3 Estimation and inference

### 3.1 Estimation

Define the *propensity score* and *regression function*, respectively, as

$$\pi^{(a)}(x) = \mathbb{P}[A = a \mid X = x] = \mathbb{E}[\mathbb{1}\{A = a\} \mid X = x], \quad (2)$$

$$\mu^{(a)}(x) = \mathbb{E}[\mathcal{Y}^{(a)} \mid X = x, A = a], \quad (3)$$

and denote their estimates by  $\hat{\pi}^{(a)}$  and  $\hat{\mu}^{(a)}$ . Notice that the techniques or algorithms employed to produce such estimates are arbitrary; often, logistic regression or random forest classifiers are used to compute  $\hat{\pi}^{(a)}$ , while complex nonparametric tools, such as neural networks, can be employed in the estimation of  $\hat{\mu}^{(a)}$ . Finally, define the *case-corrected regression function* as

$$\gamma^{(a)}(\mathcal{D}) = \mu^{(a)}(X) + \frac{\mathbb{1}\{A = a\}(\mathcal{Y}^{(a)} - \mu^{(a)}(X))}{\pi^{(a)}(X)} = \begin{cases} \mu^{(a)}(X) + \frac{\mathcal{Y}^{(a)} - \mu^{(a)}(X)}{\pi^{(a)}(X)} & \text{if } A = a \\ \mu^{(a)}(X) & \text{if } A \neq a. \end{cases} \quad (4)$$

The following Lemma is pivotal in the derivation of the DR-FoS estimator.

**Lemma 2** *Under Assumptions 1 (identifiability), the FATE defined in Eq. 1 can be rewritten as:*

$$\beta = \mathbb{E} \left[ \gamma^{(1)}(\mathcal{D}) - \gamma^{(0)}(\mathcal{D}) \right]. \quad (5)$$

We defer the proof of this and subsequent claims to Appendix Section A.

Let  $\hat{\mathbb{P}}$  denote the sample distribution on which  $\hat{\mu}^{(a)}$  and  $\hat{\pi}^{(a)}$  are produced. We assume to have access to a separate sample distribution  $\mathbb{P}_n$  independent of  $\hat{\mathbb{P}}$ , and define the *one-step* functional augmented inverse probability weighting estimator  $\hat{\beta}_{\text{DR-FoS}}$  as

$$\begin{aligned} \hat{\beta}_{\text{DR-FoS}} &= \mathbb{P}_n \left[ \hat{\gamma}^{(1)}(\mathcal{D}) - \hat{\gamma}^{(0)}(\mathcal{D}) \right] \\ &= \frac{1}{n} \sum_{i=1}^n \left( \hat{\gamma}^{(1)}(\mathcal{D}_i) - \hat{\gamma}^{(0)}(\mathcal{D}_i) \right) \\ &= \frac{1}{n} \sum_{i=1}^n \left[ \left( \hat{\mu}^{(1)}(X_i) + \frac{A_i(\mathcal{Y}_i - \hat{\mu}^{(1)}(X_i))}{\hat{\pi}^{(1)}(X_i)} \right) - \left( \hat{\mu}^{(0)}(X_i) + \frac{(1 - A_i)(\mathcal{Y}_i - \hat{\mu}^{(0)}(X_i))}{1 - \hat{\pi}^{(1)}(X_i)} \right) \right]. \end{aligned} \quad (6)$$

Notice that if  $\hat{\pi}^{(a)} = \pi^{(a)}$  and  $\hat{\mu}^{(a)} \neq \mu^{(a)}$ , we have  $\mathbb{E} \left[ \hat{\beta}_{\text{DR-FoS}} \right] = \beta$ . Similarly, if  $\hat{\pi}^{(a)} \neq \pi^{(a)}$  and  $\hat{\mu}^{(a)} = \mu^{(a)}$ , we again have  $\mathbb{E} \left[ \hat{\beta}_{\text{DR-FoS}} \right] = \beta$ . In other words,  $\hat{\beta}_{\text{DR-FoS}}$  remains unbiased as long as either the propensity score model  $\hat{\pi}^{(a)}$  or the outcome regression model  $\hat{\mu}^{(a)}$  is correctly specified. This illustrates the *double robustness* of the estimator, a property that we will further explore under additional assumptions on convergence rates later in the paper.

**Remark 3** *The derivation of  $\hat{\beta}_{\text{DR-FoS}}$  exploits the influence functions of the target of inference  $\beta$ . Unlike in standard semiparametric theory (Tsiatis, 2006), the influence functions here are infinite-dimensional and take the form*

$$\varphi(\mathcal{D}) = \gamma^{(1)}(\mathcal{D}) - \gamma^{(0)}(\mathcal{D}) - \beta. \quad (7)$$

*However, perhaps surprisingly, in our developments we never need these infinite-dimensional functions to be well-defined. Instead, we only require that their projections – which are finite-dimensional random vectors – satisfy some consistency conditions. We believe that the study of infinite-dimensional influence functions deserves a focus on its own, but it is outside the scope of this paper.*

**Remark 4** *The framework developed so far can be leveraged to enable DR-FoS to attain further robustness. In fact, multiple base models can be fitted for both the propensity score and the outcome regression, with their predictions subsequently combined using techniques such as stacking (Pavlyshenko, 2018) or SuperLearner (Van der Laan et al., 2007). Then, these ensemble models can be incorporated into Eq. 6. By adopting this approach, the DR-FoS procedure remains consistent as long as at least one among the base models is consistent, providing further protection against model misspecification.*

A separate independent sample  $\mathbb{P}_n$  can be obtained by splitting the data. To obtain full sample size efficiency, we exploit *cross-fitting*. Cross-fitting works as follows. We first randomly split the observations  $\{\mathcal{D}_1, \dots, \mathcal{D}_n\}$  into  $J$  disjoint folds (without loss of generality, we assume that the number of observations  $n$  is divisible by  $J$ ). For each  $j = 1, \dots, J$  we form  $\hat{\mathbb{P}}^{[-j]}$  with all but the  $j$ -th fold, and  $\mathbb{P}_n^{[j]}$  with the  $j$ -th fold. Then, we learn  $\hat{\mu}^{(a)[-j]}$  and  $\hat{\pi}^{(a)[-j]}$  on  $\hat{\mathbb{P}}^{[-j]}$ , and evaluate  $\hat{\beta}_{\text{DR-FoS}}^{[j]}$  on  $\mathbb{P}_n^{[j]}$ . Finally, we average to obtain our *cross-fitted* estimator as

$$\hat{\beta}_{\text{DR-FoS}} = \frac{1}{J} \sum_{j=1}^J \hat{\beta}_{\text{DR-FoS}}^{[j]} . \quad (8)$$

**Remark 5** *The causal inference problem we are considering naturally resembles the missing data setup with two levels of missingness (Tsiatis, 2006). Let  $R$  denote the missingness indicator. In this case, the prototypical observed data can be represented as  $\mathcal{D} = (X, R, R\mathcal{Y})$ . The term  $R\mathcal{Y}$  highlights that we only observe  $\mathcal{Y}$  when  $R = 1$ . Under the assumptions of missing at random (MAR), that is  $\mathcal{Y} \perp\!\!\!\perp R \mid X$ , and positivity, i.e.  $0 < \mathbb{P}[R = 1 \mid X = x] < 1$  for every  $x$  almost surely, the target  $\beta = \mathbb{E}[\mathcal{Y}]$  can be identified, and then efficiently estimated using  $\hat{\beta}_{\text{DR-FoS}} = n^{-1} \sum_{i=1}^n \left( \hat{\mu}(X_i) + \frac{A_i(\mathcal{Y}_i - \hat{\mu}(X_i))}{\hat{\pi}(X_i)} \right)$ , where  $\hat{\pi}$  is an estimator of  $\mathbb{P}[R = 1 \mid X = x]$  and  $\hat{\mu}$  is an estimator of  $\mathbb{E}[\mathcal{Y} \mid X, R = 1]$ .*

### 3.2 Inference

In the well-known scalar response setting, standard semiparametric theory shows that the ATE estimator, under some conditions, is asymptotically normal (Kennedy, 2024). Therefore, we can show that even when the outcome is functional, *pointwise asymptotic normality* holds if similar conditions are satisfied (see Corollary 11 below). However, this does not imply simultaneous guarantees over the continuous domain of our functional outcome. Thus, we rely on convergence of probability measures in the space of continuous functions to show that our estimator possesses an asymptotic Gaussian process behaviour. Then, we exploit this fact to build confidence bands that guarantee simultaneous coverage, both based on the parametric bootstrap approach proposed by Pini and Vantini (2017) and on the critical value functions approach proposed by Liebl and Reimherr (2023).

Compared to the classical causal inference framework where the outcome is real-valued, the problem we are tackling here requires additional structure. In particular, we need to introduce more notation and assumptions. First, for any  $t \in \mathcal{T}$ , we denote the one-dimensional projection of  $\beta$  and  $\hat{\beta}_{\text{DR-FoS}}$  at  $t$  as  $\beta(t)$  and  $\hat{\beta}_{\text{DR-FoS}}(t)$ , respectively. Similarly, we denote the one-dimensional projection of  $\varphi(\mathcal{D})$  and  $\hat{\varphi}(\mathcal{D})$  at  $t$  as  $\varphi(\mathcal{D}; t)$  and  $\hat{\varphi}(\mathcal{D}; t)$ . Next, we consider the following assumptions.

**Assumption 6 (Inference)** *Let the number of cross-fitting folds be fixed at  $J$ , and assume that:*

- a. *For each  $j \in \{1, \dots, J\}$ , and for every one-dimensional projection  $\varphi(\mathcal{D}; t)$ , one has*

$$\hat{\varphi}^{[-j]}(\mathcal{D}; t) \xrightarrow{\mathbb{L}^2} \varphi(\mathcal{D}; t) .$$

b. For every one-dimensional projection  $\varphi(\mathcal{D}; t)$ , one has

$$\sqrt{n} \sum_{j=1}^J R_2^{[j]} = o_{\mathbb{P}}(1),$$

where  $R_2^{[j]} = \hat{\beta}_{\text{DR-FoS}}^{[-j]}(t) - \beta(t) + \int \hat{\varphi}^{[-j]}(\mathcal{D}; t) d\mathbb{P}$ .

c. Given  $\xi > 0$ ,  $\hat{\pi}^{(a)}$  is bounded away from  $\xi$  and  $1 - \xi$  with probability 1.

d. For any  $\delta > 0$ , the functional outcome satisfies

$$\mathbb{E} \left[ \sup_{|s-t| \leq \delta} |\mathcal{Y}(s) - \mathcal{Y}(t)| \right] \leq L\delta^\tau \quad (9)$$

for some constants  $L \geq 0$  and  $\tau > 0$ .

e. For any  $\delta > 0$ , and for  $a \in \{0, 1\}$ , the estimated regression function satisfies

$$\mathbb{E} \left[ \sup_{|s-t| \leq \delta} |\hat{\mu}^{(a)}(s) - \hat{\mu}^{(a)}(t)| \right] \leq L^{(a)}\delta^\tau \quad (10)$$

for some constants  $L^{(a)} \geq 0$  and  $\tau > 0$ .

**Remark 7** Taking the number of folds as fixed to rule out undesired asymptotic behaviors of cross-fitting, as well as Assumptions **a**, **b** and **c**, are standard in causal inference – see Kennedy (2024). In particular, Assumptions **a**, **b**, and **c** are required to control the empirical process and the remainder term arising from the Von Mises expansion in Lemma 10. Notice that we do not require any condition on the influence functions  $\varphi(\mathcal{D})$ . We only need first-order assumptions on the consistency of influence function estimators  $\hat{\varphi}(\mathcal{D}; t)$ , as is standard in the literature with scalar outcomes. See Remark 8 below for additional comments on assumption **b**. Assumption **d** is much lighter than what is usually required in the functional data literature. For example, the assumption of Dette et al. (2020) on Lipschitz sample paths, i.e.  $|\mathcal{Y}(s) - \mathcal{Y}(t)| \leq L'|s - t|$ , clearly implies ours with  $L' = L$  and  $\tau = 1$ . Moreover, we stress the fact that we do not require the functional outcome to be in a Hilbert space. Finally, Assumption **e** is a regularity condition on the regression function estimator. This can be superfluous depending on the methodology at hand. See Example 9 below, where assumption **d** implies **e**.

**Remark 8** The remainder term in Assumption **b** can be bounded by the product of the norms of the distance between true and estimated nuisance functions. In fact, by direct evaluation of  $R_2$ , we can show that

$$\begin{aligned} R_2 = & \int \left| \frac{1}{\pi^{(1)}(X)} - \frac{1}{\hat{\pi}^{(1)}(X)} \right| \left| \mu^{(1)}(X; t) - \hat{\mu}^{(1)}(X; t) \right| \pi^{(1)}(X) d\mathbb{P} \\ & - \int \left| \frac{1}{1 - \pi^{(1)}(X)} - \frac{1}{1 - \hat{\pi}^{(1)}(X)} \right| \left| \mu^{(0)}(X; t) - \hat{\mu}^{(0)}(X; t) \right| (1 - \pi^{(1)}(X)) d\mathbb{P}. \end{aligned} \quad (11)$$

Given that, by Assumption **c**,  $\hat{\pi}^{(1)}(X) \geq \varepsilon$  with probability 1, by Cauchy-Schwarz we have

$$\begin{aligned}
 |R_2| &\leq \frac{1}{\varepsilon} \int \left| \pi^{(1)}(X) - \hat{\pi}^{(1)}(X) \right| \left| \mu^{(1)}(X; t) - \hat{\mu}^{(1)}(X; t) \right| d\mathbb{P} \\
 &\quad - \frac{1}{\varepsilon} \int \left| \hat{\pi}^{(1)}(X) - \pi^{(1)}(X) \right| \left| \mu^{(0)}(X; t) - \hat{\mu}^{(0)}(X; t) \right| d\mathbb{P} \\
 &\leq \frac{1}{\varepsilon} \mathbb{E} \left[ \pi^{(1)}(X) - \hat{\pi}^{(1)}(X) \right] \left( \mathbb{E} \left[ \mu^{(1)}(X; t) - \hat{\mu}^{(1)}(X; t) \right] - \mathbb{E} \left[ \mu^{(0)}(X; t) - \hat{\mu}^{(0)}(X; t) \right] \right).
 \end{aligned} \tag{12}$$

The fact that the remainder is bounded by the product of the norms of the distance between true and estimated quantities is also referred to as mixed bias, product bias, or strong double-robustness property (Wager, 2024), as opposed to the weak double-robustness property presented in the main text (see Section 3.1). This property implies that the rate at which the remainder converges to 0 is given by the product of the rates at which the estimators converge to truth. This turns out to be particularly useful in our context. In fact, in several applications it would be reasonable to assume that the estimation of the regression functions  $\mu^{(a)}(X)$ ,  $a \in \{0, 1\}$  is a more complex task than the estimation of  $\pi^{(1)}(X)$ . Indeed,  $\mu^{(a)}$  maps a vector of size  $p$  into a function in  $C(\mathcal{T})$ ;  $\pi^{(a)}$  maps the same vector into a variable supported in  $(0, 1)$ . If the rate of convergence of  $\hat{\pi}^{(1)}$  were parametric (i.e.  $n^{-1/2}$ ), then any rate of convergence for  $\hat{\mu}^{(a)}$  would suffice to guarantee the convergence of DR-FoS to a Gaussian process. See Kennedy (2024) for additional comments on this problem.

**Example 9 (Assumption **e** can be superfluous)** Let  $\mathbb{Y} = (\mathcal{Y}_1, \dots, \mathcal{Y}_n)^T$  and, similarly,  $\mathbb{X} = (X_1, \dots, X_n)^T$ . The standard function-on-scalar OLS estimator is given by

$$\hat{\theta}_{OLS} = (\mathbb{X}^T \mathbb{X})^{-1} \mathbb{X}^T \mathbb{Y}. \tag{13}$$

The estimated regression function is thus

$$\hat{\mu}(X) = X \hat{\theta}_{OLS}. \tag{14}$$

Clearly, with a slight abuse of notation, we have that

$$\begin{aligned}
 \mathbb{E} \left[ \sup_{|s-t| \leq \delta} |\hat{\mu}(s) - \hat{\mu}(t)| \right] &= \mathbb{E} \left[ X \mathbb{E} \left[ \sup_{|s-t| \leq \delta} |\hat{\theta}(s) - \hat{\theta}(t)| \mid X \right] \right] \\
 &= \mathbb{E} \left[ X (\mathbb{X}^T \mathbb{X})^{-1} \mathbb{X}^T \mathbb{E} \left[ \sup_{|s-t| \leq \delta} |\mathbb{Y}(s) - \mathbb{Y}(t)| \right] \right] \\
 &\leq L'' |s - t|^\tau,
 \end{aligned} \tag{15}$$

where  $L'' = L \mathbb{E} [X (\mathbb{X}^T \mathbb{X})^{-1} \mathbb{X}^T]$ . An extension to linear smoothers goes through a similar line of reasoning. We stress that Assumption **6d** imposes regularity on the outcome process  $\mathcal{Y}$  itself, independent of the estimation procedure. In contrast, Assumption **6e** is a condition on the estimated regression functions  $\hat{\mu}^{(a)}$ . In practice, methods like linear smoothers will ensure that  $\hat{\mu}^{(a)}$  inherits sufficient smoothness from the estimation method itself.

**Lemma 10 (Asymptotic normality of finite dimensional projections)** *Let  $k \in \mathbb{N}$  and  $t_1, \dots, t_k \in \mathcal{T}$  be fixed. Define  $\hat{B}_{t_1, \dots, t_k} = \left( \hat{\beta}_{DR-FoS}(t_1), \dots, \hat{\beta}_{DR-FoS}(t_k) \right)^T$  and  $B_{t_1, \dots, t_k} = (\beta(t_1), \dots, \beta(t_k))^T$ . Under Assumptions 1 (identifiability) and 6 (inference), one has*

$$\sqrt{n} \left( \hat{B}_{t_1, \dots, t_k} - B_{t_1, \dots, t_k} \right) \rightsquigarrow \mathcal{N} \left( 0, \Sigma_{t_1, \dots, t_k} \right), \quad (16)$$

where  $v_{t_1, \dots, t_k}(\mathcal{D}) = (\varphi(\mathcal{D}; t_1), \dots, \varphi(\mathcal{D}; t_k))^T$  and  $\Sigma_{t_1, \dots, t_k} = \mathbb{E} \left[ v_{t_1, \dots, t_k}(\mathcal{D}) v_{t_1, \dots, t_k}(\mathcal{D})^T \right]$ .

The claim in Lemma 10 is similar to the one in Theorem 5.31 of Van der Vaart (2000), with the notable difference that, by exploiting cross-fitting, we greatly reduce the Donsker-type assumptions on population and estimated quantities. Our claim also resembles Lemma C.8 in Martinez Taboada et al. (2023). A similar, more general, result is also found in Lemma 3 of Kennedy et al. (2023). As stated in the following Corollary, Lemma 10 also guarantees pointwise asymptotic normality.

**Corollary 11 (Pointwise Asymptotic normality)** *Let  $t \in \mathcal{T}$  be fixed. Under the assumptions of Lemma 10, one has*

$$\sqrt{n} \left( \hat{\beta}_{DR-FoS}(t) - \beta(t) \right) \rightsquigarrow \mathcal{N} \left( 0, \Sigma_t \right), \quad (17)$$

where  $\Sigma_t = \mathbb{V}[\varphi(\mathcal{D}; t)] = \mathbb{E}[\varphi^2(\mathcal{D}; t)]$ .

We are now ready to present the main result of this Section, which will be pivotal in the construction of simultaneous confidence bands required to perform inference. It informally states that the asymptotic distribution of  $\hat{\beta}_{DR-FoS}$  is a Gaussian process.

**Theorem 12 (Convergence to Gaussian process)** *Under Assumptions 1 (identifiability) and 6 (inference), one has*

$$\sqrt{n} \left( \hat{\beta}_{DR-FoS} - \beta \right) \rightsquigarrow \mathcal{GP}(0, \Sigma), \quad (18)$$

where  $\Sigma(s, t) = \mathbb{E}[\varphi(\mathcal{D}; s)\varphi(\mathcal{D}; t)]$ .

**Remark 13** *Our CLT can be extended using the tools introduced in Dette et al. (2020) to accommodate dependent and non-identically distributed data. However, we note that restricting ourselves to the i.i.d. case, as presented here, allows us to employ a less stringent condition on the continuity of sample paths. Also, since our objective is to set the stage for extending standard causal inference approaches (which usually assume i.i.d. data) to functional data analysis, considering the i.i.d. case seems fully justified.*

**Remark 14** *Inference for the functional average treatment effect using DR-FoS, by exploiting influence functions and cross-splitting, requires very mild assumptions compared to the proposal of Liu et al. (2024). In fact, we make virtually no assumption about the shape and complexity of the population regression function and propensity score. Instead, Liu et al. (2024) impose strong modeling constraints on the regression function (which is assumed to*

be linear) and on the propensity score (which is assumed to be logistic). They also require the usual regularity conditions for asymptotic normality of  $M$ -estimators. Moreover, in our set of assumptions for inference, we only require that functional outcomes satisfy an expected Hölder condition, while Liu et al. (2024) require the much more stringent assumption that outcomes be defined in a Hilbert space, where standard asymptotic theory is applicable.

Endowed with the previous result, we can now build confidence bands for inference. An elegant pivotal approach, borrowed by Liebl and Reimherr (2023), requires the estimation of a critical value function  $\hat{u}_{\alpha/2}^*$ , which guarantees control over the false positive rate. We refer the interested reader to Liebl and Reimherr (2023) for additional details and note that, while this approach possesses a variety of virtues, it also requires an additional assumption on the covariance of the process.

**Proposition 15 (Simultaneous Coverage)** *Assume that the estimated covariance function  $\hat{\Sigma}$  is one-time differentiable, and let the function  $\hat{\sigma}^2$  denote its main diagonal. The  $(1 - \alpha)$  confidence band*

$$C_\alpha = [\hat{\beta}_{DR-FoS}^l, \hat{\beta}_{DR-FoS}^u] = \hat{\beta}_{DR-FoS} \pm \frac{1}{\sqrt{n}} \hat{u}_{\alpha/2}^* \hat{\sigma} \quad (19)$$

*provides simultaneous coverage.*

Another assumption-lean approach to construct simultaneous confidence bands is based on the parametric bootstrap (Pini and Vantini, 2017). This approach consists in repeatedly sampling from the process, and estimating quantiles accordingly, without any additional assumption on the covariance function. In symbols, the interval takes the form  $C_\alpha = [\hat{\beta}_{\alpha/2}, \hat{\beta}_{1-\alpha/2}]$ , where  $\hat{\beta}_{\alpha/2}$  and  $\hat{\beta}_{1-\alpha/2}$  indicate the estimated  $\alpha/2$  and  $1 - \alpha/2$  quantiles, respectively. Given its ease of implementation, and the fact that it requires no additional assumptions, we adopt the parametric bootstrap approach in the following Sections.

**Remark 16** *Our analysis relies on the Banach space  $C(\mathcal{T})$  equipped with the sup-norm. This choice is helpful to construct valid simultaneous confidence bands, as it ensures control over the maximum deviation of the estimated treatment effect across the entire domain  $\mathcal{T}$ . We acknowledge that this entails a stronger topological constraint compared to Hilbert space approaches (e.g., using the  $\mathbb{L}^2$  norm), where convergence rates require fewer assumptions (Van Der Vaart and Wellner, 1996). As highlighted by Singh et al. (2024), estimators prioritizing local smoothing can achieve higher pointwise accuracy and may adapt better to local irregularities than global sup-norm approaches. However, such methods generally do not provide the uniform coverage guarantees required for simultaneous inference. By assuming expected Hölder continuity (Assumption 6d), DR-FoS secures a parametric  $\sqrt{n}$ -convergence rate in the supremum norm, effectively trading stronger regularity conditions for the ability to perform valid global inference.*

## 4 Simulation study

We employ synthetic data to investigate and compare performance of DR-FoS in both well-specified and misspecified scenarios. We first generate the true regression functions according to the model

$$\mu^{(a)} = a\beta + \rho, \quad a \in \{0, 1\}, \quad (20)$$

where the FATE  $\beta$  and the baseline function  $\rho$  are drawn from a 0 mean Gaussian process with a Matern covariance function (Cressie and Huang, 1999) of the form

$$C(s, t) = \frac{\eta^2}{\Gamma(\nu)2^{\nu-1}} \left( \frac{\sqrt{2\nu}}{l} |s - t| \right)^\nu \chi_\nu \left( \frac{\sqrt{2\nu}}{l} |s - t| \right). \quad (21)$$

Here  $\chi_\nu$  is a modified Bessel function, and we set the parameters to  $l = 0.25$ ,  $\nu = 3.5$ , and  $\eta^2 = 1$ . We then generate the potential outcomes as

$$\mathcal{Y}_i^{(a)} = \mu^{(a)} + \varepsilon_i, \quad (22)$$

where the error  $\varepsilon_i$  is again drawn from a 0 mean Gaussian process with a Matern covariance function; here we set  $l = 0.25$ ,  $\nu = 2.5$ , and  $\eta = \mathbb{V}[A_i\beta + \rho]/10$ , where with a slight abuse of notation  $\mathbb{V}[A_i\beta + \rho]$  indicates the global (pooled over time) variance of the signal  $A_i\beta + \rho$ . This roughly ensures that the pooled signal-to-noise ratio is approximately 1. The observed outcome is thus

$$\mathcal{Y}_i = A_i\mathcal{Y}_i^{(1)} + (1 - A_i)\mathcal{Y}_i^{(0)}, \quad (23)$$

where  $A_i \sim \text{Ber}(\tilde{p})$ ,  $\tilde{p} = 0.5$ .

We control the degree of misspecification in the estimated propensity score and in the estimated regression functions through the parameters  $\alpha_\pi$  and  $\alpha_\mu$ , respectively. In particular we define the estimated propensity score as

$$\hat{\pi}_i = \alpha_\pi U_i + (1 - \alpha_\pi)\tilde{p}, \quad (24)$$

where  $U_i$  is sampled from a balanced mixture of two normal distributions. The first normal has mean 0.2 and standard deviation 0.1; the second normal has mean 0.8 and standard deviation 0.1. The mixture is truncated in the interval  $[0.02, 0.98]$ . Similarly, we define the estimated regression functions as

$$\hat{\mu}_i^{(a)} = \alpha_\mu \mathcal{U}_i + (1 - \alpha_\mu)\mu^{(a)}, \quad (25)$$

where  $\mathcal{U}_i$  is drawn from a 0 mean Gaussian process with Matern covariance function with parameters  $l = 0.25$ ,  $\nu = 2.5$ ,  $\eta^2 = 1$ . This simulation structure allows us to study and compare the performance of the various FATE estimators under different misspecification scenarios, without concerning ourselves with potential biases introduced by the methods used to produce  $\hat{\mu}^{(a)}$  and  $\hat{\pi}$ . In fact,  $\alpha_\mu$  and  $\alpha_\pi$  control the convex combinations between true and random quantities. The lower the values of  $\alpha_\mu$  and  $\alpha_\pi$ , the stronger the correspondence between true quantities and estimates; the higher the values of  $\alpha_\mu$  and  $\alpha_\pi$ , the more the estimates are pulled towards random directions, progressively injecting bias. In a way,  $\alpha_\pi$  and  $\alpha_\mu$  can be interpreted as proxies of the rate of convergence of  $\hat{\pi}$  and  $\hat{\mu}^{(a)}$  to their corresponding population quantities – see Das et al. (2024) for a more explicit characterization. For each simulation scenario, we set  $n = 5000$ ,  $\alpha_\pi, \alpha_\mu \in \{0, 0.25, 0.5, 0.75, 1\}$  and run experiments with 50 different seeds.

We perform extensive simulations to compare DR-FoS with two commonly used FATE estimators: the *outcome regression* estimator defined as

$$\hat{\beta}_{\text{OR}} = \frac{1}{n} \sum_{i=1}^n \left[ \hat{\mu}_i^{(1)} - \hat{\mu}_i^{(0)} \right], \quad (26)$$

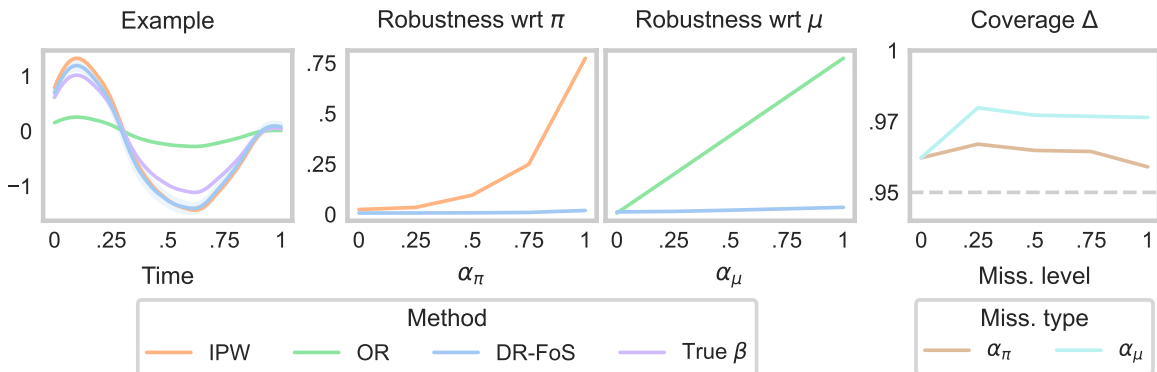


Figure 1: Simulation results based on the data generating process described in Section 4. The first panel (leftmost) shows an example of true FATE  $\beta$  (purple) as generated by our simulation scheme, and the estimates provided by IPW (orange), OR (green) and DR-FoS (blue) – together with simultaneous confidence bands around the latter. In this example we set  $\alpha_\mu = 0.25$  and  $\alpha_\pi = 0.75$ . The second panel shows the average (across simulation replicates) estimation error as captured by the MSE when the estimated propensity score is increasingly corrupted by random noise, and the regression functions are well-specified ( $\alpha_\mu = 0$ ,  $\alpha_\pi \neq 0$ ). While DR-FoS (blue) maintains excellent performance, IPW (orange) performs progressively worse, as expected. The third panel displays the opposite situation, where the estimated regression functions are increasingly corrupted by random noise and the propensity score is well-specified ( $\alpha_\mu \neq 0$ ,  $\alpha_\pi = 0$ ). Again, the performance of DR-FoS (blue) remains excellent, while the performance of OR (green) progressively deteriorates. Finally, the last panel (rightmost) shows the average coverage levels achieved under misspecifications of the regression functions (light blue,  $\alpha_\pi = 0$ ) and of the propensity score (brown,  $\alpha_\mu = 0$ ). The grey dashed line represents the nominal 95% coverage level.

and the *inverse probability weighting* estimator defined as

$$\hat{\beta}_{\text{IPW}} = \frac{1}{n} \sum_{i=1}^n \left[ \frac{A_i \mathcal{Y}_i}{\hat{\pi}_i^{(1)}} - \frac{(1 - A_i) \mathcal{Y}_i}{1 - \hat{\pi}_i^{(1)}} \right]. \quad (27)$$

The latter estimator is well known in the scalar setting, but to the best of our knowledge it has never been analyzed in the functional data literature. In Appendix Section B we therefore study its properties and asymptotic behavior.

We assess performance in terms of estimation accuracy and inferential coverage. To measure accuracy, we compute the mean squared error under the  $\mathbb{L}^2$  distance between the true  $\beta$  and its estimate  $\hat{\beta}$ , i.e.  $\text{MSE}(\hat{\beta}) = \int (\beta(t) - \hat{\beta}(t))^2 dt$ . To measure actual coverage, we evaluate the percentage  $\Delta$  of the domain of  $\beta$  that falls into the parametric bootstrap simultaneous coverage bands, i.e.  $\Delta = \int \mathbb{1}\{\beta(t) \in [\hat{\beta}^l(t), \hat{\beta}^u(t)]\} dt$ .

Figure 1 shows an example of true FATE alongside its estimates using OR, IPW, and DR-FoS, for one specific scenario (first panel; the underlying simulation parameters are re-

ported in the caption). Figure 1 also displays the performance of the various estimators based on the metrics described above. In a well-specified scenario, all estimators are comparable. However, when random noise corrupts either the propensity score (second panel) or the regression function (third panel), the performance of IPW and OR markedly deteriorates. In contrast, DR-FoS consistently achieves high accuracy in both cases, provided at least one of the two models – the propensity score or the regression function – is well-specified. The fourth panel displays coverage performance. The simultaneous confidence bands effectively control the type I error, ensuring the nominal 95% coverage level. However, under both misspecification scenarios, DR-FoS appears to exhibit some overcoverage. In Appendix Section C we report results for additional simulation scenarios where both models are misspecified at the same time and where we introduce discontinuities to evaluate the behavior of DR-FoS simultaneous confidence bands when the continuity assumption is not satisfied. There, we also report further, more standard simulation scenarios where we explicitly model the data generating process and the nuisance functions, such as the linear case in which  $\mu^{(a)}(X_i) = \sum_{j=1}^p X_{ij}\theta_j^{(a)}$  for some scalar variables  $X_{ij}$  and functional coefficients  $\theta_j^{(a)}$ ; notably, even in these cases, DR-FoS matches or outperforms the other estimators.

## 5 SHARE application

To demonstrate the use of DR-FoS, we apply it to the SHARE (*Survey of Health, Aging and Retirement in Europe*) dataset (Alcser et al., 2005). SHARE is a research infrastructure that aims to investigate the effects of health, social, economic, and environmental policies on the life course of European citizens (Bergmann et al., 2017; Börsch-Supan et al., 2013; Börsch-Supan, 2020). SHARE is a longitudinal study, where the same subjects are followed over multiple years. Specifically, eight surveys – or “waves” – were conducted from 2004 to 2020.

Specifically, we employ the proposed estimator to investigate the causal effect of chronic conditions on longitudinal indicators of quality of life. We first preprocess data following the steps described in Boschi et al. (2024a). We focus on the 1518 subjects who participated in at least seven out of the eight waves, ensuring a sufficient number of measurements for reliable curve estimation. We investigate a subset of the variables from the EasySHARE dataset (Gruber et al., 2014), a preprocessed version of the SHARE data. For each subject, we consider: two functional indicators of quality of life – a mobility index and the Quality of Life Scale (CASP) (Hyde et al., 2003), measured over 192 months; two chronic diseases – high cholesterol and hypertension; and a variety of socio-demographic and healthcare factors (see Table 1). While some of these variables are characterized by values that change over time (e.g., CASP and mobility index) and are suitable for a functional representation, others are scalar (e.g., education years) or categorical (e.g., gender) and do not evolve over different waves. We smooth time-varying variables using cubic *B-splines* with knots at each survey date and roughness penalty on the curves second derivative (Ramsay and Silverman, 2005). For each curve, the smoothing parameter is selected by minimizing the average generalized cross-validation error (Craven and Wahba, 1978). Although the survey dates and the amount of measurements may vary across subjects, the functional representation

Table 1: Variables employed in the SHARE application study.

Variable name	Type	Usage
Hypertension condition	Binary	Treatment
High cholesterol	Binary	Treatment
Age	Scalar	Covariate
Years of education	Scalar	Covariate
Score of first numeracy test	Scalar	Covariate
Gender	Binary	Covariate
Smoke	Binary	Covariate
Vaccinations during childhood	Binary	Covariate
Mobility index	Functional	Outcome
CASP	Functional	Outcome

provides a natural imputation for missing values and facilitates the comparison of different statistical units across the entire temporal domain.

Following the logic of the counterfactual model, we define the causal effect of a chronic disease on a quality of life indicator as the expected difference between the functional outcome if a subject had, or did not have, the chronic disease. Therefore, we first form treatment groups identifying subjects who present chronic conditions at the beginning of the study. Similarly, we form control groups identifying subjects who never develop chronic conditions throughout the study period. We acknowledge that this retrospective definition of the control group introduces a form of selection or immortal-time bias since it utilizes information post-baseline (the absence of the condition throughout the study). Therefore, for this illustrative application, the estimand should be interpreted as the average difference in functional trajectories conditional on long-term disease-free status versus chronic disease status at baseline, rather than a causal effect of incident treatment. We acknowledge that more complex causal frameworks, like g-computation or Marginal Structural Models (MSMs), can deal with time-varying treatments or censoring by handling time-dependent confounding and estimating dynamic treatment effects (Robins, 1986; Tsiatis, 2006). However, these approaches cannot be readily applied to functional data. For high cholesterol, we have 313 subjects in the treatment group and 747 in the control group. Similarly, for hypertension, we have 419 treated subjects and 577 controls.

For each combination of chronic disease and functional outcome, we then fit DR-FoS using a function-on-scalar least squares specification for the regression function  $\hat{\mu}^{(a)}$ , and logistic regression for the propensity score  $\hat{\pi}^{(a)}$  (additional implementations with more sophisticated nuisance models can be found in Appendix Section D). No time-varying or post-baseline variables beyond the cohort definition are used in the propensity score or outcome models. We employ cross-fitting with 5 balanced folds. Results are shown in Figure 2. The two chronic conditions both have a positive and statistically significant effect on the mobility index across the entire time period. Thus, chronic conditions adversely affect mobility (a higher mobility index corresponds to reduced mobility). Similarly, the effects of both chronic conditions on CASP are negative and statistically significant throughout the time period, highlighting a detrimental impact on quality of life as measured by this metric. The

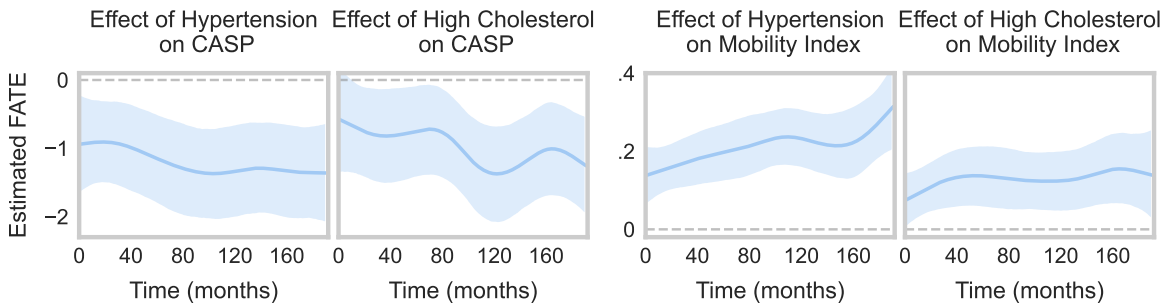


Figure 2: SHARE application results. Each panel displays a different estimated causal effect. Blue continuous lines correspond to DR-FoS estimates; blue bands are 95% asymptotic simultaneous confidence bands obtained by repeatedly sampling from the Gaussian process; grey dotted horizontal lines correspond to 0.

impacts of chronic conditions on functional outcomes also appear to increase in magnitude over time. Thus, as individuals age, the adverse effects of chronic conditions on their quality of life become progressively more pronounced. Taken together, these findings demonstrate the utility of DR-FoS in real-world applications, and its ability to enhance our understanding of complex phenomena.

## 6 Conclusion

In this paper, we introduced DR-FoS, a novel estimator for the Functional Average Treatment Effect (FATE) in observational settings with functional outcomes. By leveraging double robustness, DR-FoS offers consistent estimation even when the outcome model, or alternatively the treatment assignment model, is misspecified. This desirable feature ensures that our methodology is robust to potential inaccuracies in the modeling assumptions, a critical advantage in practical applications where accurate, or even just reasonable model specifications are rarely guaranteed.

Our contributions are both theoretical and relevant for practitioners. We rigorously establish the theoretical properties of DR-FoS, proving its convergence to a Gaussian process under weak assumptions. This allows us to pursue pointwise inference, as well as to construct simultaneous confidence bands, providing a comprehensive inferential framework for functional treatment effects. The methodology is versatile, leveraging modern techniques in functional data analysis and causal inference while maintaining computational efficiency.

Through extensive simulations, we show that DR-FoS outperforms commonly used alternatives, particularly under scenarios of model misspecification. These results highlight the practical utility of our approach in functional data settings, offering researchers a reliable tool for causal inference in complex, high-dimensional domains. Additionally, the application to the SHARE dataset underscores the flexibility and relevance of DR-FoS in addressing scientific questions that involve functional outcomes.

We envision several directions for future work. First, extending the methodology to more complex causal structures, such as scalar-on-function or function-on-function causal relationships, where the treatment is a continuous variable, represents a promising direction

for further investigation (Tan et al., 2025). Additionally, the assumptions underpinning the convergence to a Gaussian process could be further relaxed, particularly in the context of non i.i.d. data or outcomes observed on non-standard domains. These extensions would broaden the applicability of DR-FoS and further strengthen its theoretical foundations.

In summary, DR-FoS provides a robust, efficient, and theoretically grounded approach for estimating causal effects in observational studies where outcomes are functional data. By bridging the gap between classic causal inference and functional data analysis, it sets the stage for further advancements in the analysis of complex and structured outcomes in modern scientific applications.

## Acknowledgments and Disclosure of Funding

L.T. wishes to thank Jing Lei for helpful discussions about the theoretical properties of the proposed estimator, and Antonio C. Herling Ribeiro Jr. for invaluable feedback on the simulation strategy. The work of F.C. was partially supported by the Huck Institutes of the Life Sciences at Penn State, the L’EMbeDS Department of Excellence of the Sant’Anna School of Advanced Studies, and the SMaRT CONSTRUCT project (CUP J53C24001460006, as part of FAIR, PE0000013, CUP B53C22003630006, Italian National Recovery and Resilience Plan funded by NextGenerationEU). The work of E.H.K. was supported by the NSF CAREER Award 2047444. The work of M.R. was partially supported by the NSF SES Award 1853209.

## References

- Kirsten H. Alcser, Grant Benson, Axel Barsch-Supan, Agar Brugiavini, Dimitrios Christelis, Enrica Croda, Marcel Das, Guiseppe de Luca, Janet Harkness, Patrik Hesselius, Tullio Jappelli, Hendrik Jarges, Adriaan Kalwij, Marie-Louise Kemperman, Anders Klevmarken, Oliver Lipps, Omar Paccagnella, Mario Padula, Franco Perrachi, Roberta Rainato, Arthur van Soest, Bengt Swensson, Corrie Vis, Guglielmo Weber, and Bas Weerman. *The Survey of Health, Aging, and Retirement in Europe: Methodology*. Mannheim Research Institute for the Economics of Aging (MEA), 2005.
- Michael Bergmann, Thorsten Kneip, Giuseppe De Luca, and Annette Scherpenzeel. Survey participation in the survey of health, ageing and retirement in europe (share), wave 1-6. *Munich: Munich Center for the Economics of Aging*, 2017.
- Patrick Billingsley. *Convergence of probability measures*. John Wiley & Sons, 2013.
- Axel Börsch-Supan. Survey of health, ageing and retirement in europe (share) wave 5. *Release version*, 7(0), 2020.
- Axel Börsch-Supan, Martina Brandt, Christian Hunkler, Thorsten Kneip, Julie Korbmayer, Frederic Malter, Barbara Schaan, Stephanie Stuck, and Sabrina Zuber. Data resource profile: the survey of health, ageing and retirement in europe (share). *International journal of epidemiology*, 42(4):992–1001, 2013.

- Tobia Boschi, Jacopo Di Iorio, Lorenzo Testa, Marzia A Cremona, and Francesca Chiaromonte. Functional data analysis characterizes the shapes of the first covid-19 epidemic wave in italy. *Scientific reports*, 11(1):17054, 2021.
- Tobia Boschi, Jacopo Di Iorio, Lorenzo Testa, Marzia A Cremona, and Francesca Chiaromonte. Contrasting pre-vaccine covid-19 waves in italy through functional data analysis. *arXiv preprint arXiv:2307.09820*, 2023.
- Tobia Boschi, Francesca Bonin, Rodrigo Ordonez-Hurtado, Alessandra Pascale, and Jonathan P Epperlein. A new computationally efficient algorithm to solve feature selection for functional data classification in high-dimensional spaces. In *Forty-first International Conference on Machine Learning*, 2024a.
- Tobia Boschi, Francesca Bonin, Rodrigo Ordonez-Hurtado, Cécile Rousseau, Alessandra Pascale, and John Dinsmore. Functional graph convolutional networks: A unified multi-task and multi-modal learning framework to facilitate health and social-care insights. In *Proceedings of the Thirty-Third International Joint Conference on Artificial Intelligence, IJCAI-24*, pages 7188–7196. International Joint Conferences on Artificial Intelligence Organization, 2024b.
- Tobia Boschi, Lorenzo Testa, Francesca Chiaromonte, and Matthew Reimherr. Fasten: an efficient adaptive method for feature selection and estimation in high-dimensional functional regressions. *Journal of Computational and Graphical Statistics*, (just-accepted): 1–24, 2024c.
- Denis Bosq. *Linear processes in function spaces: theory and applications*, volume 149. Springer Science & Business Media, 2000.
- David Bruns-Smith, Oliver Dukes, Avi Feller, and Elizabeth L Ogburn. Augmented balancing weights as linear regression. *Journal of the Royal Statistical Society Series B: Statistical Methodology*, page qkaf019, 2025.
- Peter Craven and Grace Wahba. Smoothing noisy data with spline functions. *Numerische mathematik*, 31(4):377–403, 1978.
- Marzia A Cremona, Alessia Pini, Fabio Cumbo, Kateryna D Makova, Francesca Chiaromonte, and Simone Vantini. Iwtomics: testing high-resolution sequence-based ‘omics’ data at multiple locations and scales. *Bioinformatics*, 34(13):2289–2291, 2018.
- Noel Cressie and Hsin-Cheng Huang. Classes of nonseparable, spatio-temporal stationary covariance functions. *Journal of the American Statistical Association*, 94(448):1330–1339, 1999.
- Manjari Das, Edward H Kennedy, and Nicholas P Jewell. Doubly robust capture-recapture methods for estimating population size. *Journal of the American Statistical Association*, 119(546):1309–1321, 2024.
- Holger Dette, Kevin Kokot, and Alexander Aue. Functional data analysis in the banach space of continuous functions. *The Annals of Statistics*, 48(2):1168–1192, 2020.

- Kreske Ecker, Xavier de Luna, and Lina Schelin. Causal inference with a functional outcome. *Journal of the Royal Statistical Society Series C: Applied Statistics*, 73(1):221–240, 2024.
- Frédéric Ferraty. *Nonparametric functional data analysis*. Springer, 2006.
- Stefan Gruber, Christian Hunkler, and Stephanie Stuck. Generating easyshare: guidelines, structure, content and programming. Technical report, SHARE Working Paper Series 17-2014. Munich, 2014.
- Martin Hyde, Richard D Wiggins, Paul Higgs, and David B Blane. A measure of quality of life in early old age: the theory, development and properties of a needs satisfaction model (casp-19). *Aging & mental health*, 7(3):186–194, 2003.
- Francesca Ieva, Nicole Fontana, Carlo Andrea Pivato, Emanuele Di Angelantonio, and Piercesare Secchi. Enhancing causal inference in functional data: a method for estimating time-varying causal treatment effects. In *International Workshop on Functional and Operatorial Statistics*, pages 285–293. Springer, 2025.
- Guido W Imbens. Causal inference in the social sciences. *Annual Review of Statistics and Its Application*, 11, 2024.
- Yujin Jeong, Emily Fox, and Ramesh Johari. Identifying sparse treatment effects. *arXiv preprint arXiv:2404.14644*, 2024.
- Edward H Kennedy. Semiparametric doubly robust targeted double machine learning: a review. *Handbook of Statistical Methods for Precision Medicine*, pages 207–236, 2024.
- Edward H Kennedy, Shreya Kangovi, and Nandita Mitra. Estimating scaled treatment effects with multiple outcomes. *Statistical methods in medical research*, 28(4):1094–1104, 2019.
- Edward H Kennedy, Sivaraman Balakrishnan, and LA Wasserman. Semiparametric counterfactual density estimation. *Biometrika*, 110(4):875–896, 2023.
- Edward H Kennedy et al. Optimal doubly robust estimation of heterogeneous causal effects. *arXiv preprint arXiv:2004.14497*, 5, 2020.
- Piotr Kokoszka and Matthew Reimherr. *Introduction to functional data analysis*. CRC Press, 2017.
- Dominik Liebl and Matthew Reimherr. Fast and fair simultaneous confidence bands for functional parameters. *Journal of the Royal Statistical Society Series B: Statistical Methodology*, 85(3):842–868, 2023.
- Zhenhua Lin, Dehan Kong, and Linbo Wang. Causal inference on distribution functions. *Journal of the Royal Statistical Society Series B: Statistical Methodology*, 85(2):378–398, 2023.
- Xijia Liu, Kreske Ecker, Lina Schelin, and Xavier de Luna. Double robust estimation of functional outcomes with data missing at random. *arXiv preprint arXiv:2411.17224*, 2024.

- Alex Luedtke and Incheoul Chung. One-step estimation of differentiable hilbert-valued parameters. *The Annals of Statistics*, 52(4):1534–1563, 2024.
- Anton Rask Lundborg, Rajen D Shah, and Jonas Peters. Conditional independence testing in hilbert spaces with applications to functional data analysis. *Journal of the Royal Statistical Society Series B: Statistical Methodology*, 84(5):1821–1850, 2022.
- Diego Martinez Taboada, Aaditya Ramdas, and Edward Kennedy. An efficient doubly-robust test for the kernel treatment effect. *Advances in Neural Information Processing Systems*, 36:59924–59952, 2023.
- Bohdan Pavlyshenko. Using stacking approaches for machine learning models. In *2018 IEEE second international conference on data stream mining & processing (DSMP)*, pages 255–258. IEEE, 2018.
- Alessia Pini and Simone Vantini. Interval-wise testing for functional data. *Journal of Nonparametric Statistics*, 29(2):407–424, 2017.
- Mattia Prosperi, Yi Guo, Matt Sperrin, James S Koopman, Jae S Min, Xing He, Shannan Rich, Mo Wang, Iain E Buchan, and Jiang Bian. Causal inference and counterfactual prediction in machine learning for actionable healthcare. *Nature Machine Intelligence*, 2(7):369–375, 2020.
- Xin Qi and Ruiyan Luo. Function-on-function regression with thousands of predictive curves. *Journal of Multivariate Analysis*, 163:51–66, 2018.
- James O. Ramsay and B. W. Silverman. *Functional data analysis*. Springer, 2 edition, 2005.
- Yordan P Raykov, Hengrui Luo, Justin D Strait, and Wasiur R KhudaBukhsh. Kernel-based estimators for functional causal effects. *arXiv preprint arXiv:2503.05024*, 2025.
- James Robins. A new approach to causal inference in mortality studies with a sustained exposure period—application to control of the healthy worker survivor effect. *Mathematical modelling*, 7(9-12):1393–1512, 1986.
- Rahul Singh, Liyuan Xu, and Arthur Gretton. Kernel methods for causal functions: dose, heterogeneous and incremental response curves. *Biometrika*, 111(2):497–516, 2024.
- Ruoxu Tan, Wei Huang, Zheng Zhang, and Guosheng Yin. Causal effect of functional treatment. *Journal of Machine Learning Research*, 26(91):1–39, 2025.
- Barinder Thind, Sidi Wu, Richard Groenewald, and Jiguo Cao. Funcnn: An r package to fit deep neural networks using generalized input spaces. *arXiv preprint arXiv:2009.09111*, 2020.
- Anastasios A Tsiatis. *Semiparametric theory and missing data*, volume 4. Springer, 2006.
- Mark J Van Der Laan and Daniel Rubin. Targeted maximum likelihood learning. *The international journal of biostatistics*, 2(1), 2006.

Mark J Van der Laan, Eric C Polley, and Alan E Hubbard. Super learner. *Statistical applications in genetics and molecular biology*, 6(1), 2007.

Aad W Van der Vaart. *Asymptotic statistics*, volume 3. Cambridge university press, 2000.

Aad W Van Der Vaart and Jon A Wellner. Weak convergence. In *Weak convergence and empirical processes: with applications to statistics*, pages 16–28. Springer, 1996.

Hal R Varian. Causal inference in economics and marketing. *Proceedings of the National Academy of Sciences*, 113(27):7310–7315, 2016.

Stefan Wager. Causal inference: A statistical learning approach, 2024.

## Appendix A. Proofs of main results

Before presenting the proofs of the main results, we introduce additional notation to facilitate the exposition. First, for any  $k \in \mathbb{N}$  and  $t_1, \dots, t_k \in \mathcal{T}$ , we denote the  $k$ -dimensional projection vectors of  $\beta$  and  $\hat{\beta}_{\text{DR-FoS}}$  at  $(t_1, \dots, t_k)$  as  $B_{t_1, \dots, t_k} = (\beta(t_1), \dots, \beta(t_k))^T$  and  $\hat{B}_{t_1, \dots, t_k} = (\hat{\beta}_{\text{DR-FoS}}(t_1), \dots, \hat{\beta}_{\text{DR-FoS}}(t_k))^T$ , respectively. Similarly, we denote the  $k$ -dimensional projection vectors of  $\varphi(\mathcal{D})$  and  $\hat{\varphi}(\mathcal{D})$  at  $(t_1, \dots, t_k)$  as  $v_{t_1, \dots, t_k}(\mathcal{D}) = (\varphi(\mathcal{D}; t_1), \dots, \varphi(\mathcal{D}; t_k))^T$  and  $\hat{v}_{t_1, \dots, t_k}(\mathcal{D}) = (\hat{\varphi}(\mathcal{D}; t_1), \dots, \hat{\varphi}(\mathcal{D}; t_k))^T$ .

### A.1 Lemma 2

We start by showing that  $\mathbb{E}[\mathcal{Y}^{(1)}] = \mathbb{E}[\gamma^{(1)}(\mathcal{D})]$ . This is done exploiting the identifiability Assumptions 1. Indeed

$$\begin{aligned}
 \mathbb{E}[\gamma^{(1)}(\mathcal{D})] &= \mathbb{E}\left[\mu^{(1)}(X) + \frac{A(\mathcal{Y} - \mu^{(1)}(X))}{\pi^{(1)}(X)}\right] \\
 &= \mathbb{E}[\mu^{(1)}(X)] + \mathbb{E}\left[\frac{A(\mathcal{Y} - \mu^{(1)}(X))}{\pi^{(1)}(X)}\right] \\
 &= \mathbb{E}[\mathbb{E}[\mathcal{Y} | X, A = 1]] + \mathbb{E}\left[\mathbb{E}\left[\frac{A(\mathcal{Y} - \mu^{(1)}(X))}{\pi^{(1)}(X)} \mid X\right]\right] \\
 &= \mathbb{E}[\mathbb{E}[\mathcal{Y} | X, A = 1]] \\
 &= \mathbb{E}[\mathcal{Y}^{(1)}].
 \end{aligned} \tag{28}$$

A similar computation leads to  $\mathbb{E}[\mathcal{Y}^{(0)}] = \mathbb{E}[\gamma^{(0)}(\mathcal{D})]$ . Combining the two results implies the desired equality.

### A.2 Lemma 10

For simplicity, we show the result for a single cross-fitting fold. In particular, denote the distribution where  $\hat{\mu}^{(a)}$  and  $\hat{\pi}^{(a)}$  are trained as  $\hat{\mathbb{P}}$ , and the distribution where the influence functions are approximated as  $\mathbb{P}_n$ .

First, assume that  $\Sigma_{t_1, \dots, t_k} = \mathbb{E}[v_{t_1, \dots, t_k}(\mathcal{D})v_{t_1, \dots, t_k}(\mathcal{D})^T]$  is known. By the Von Mises expansion, we have:

$$\sqrt{n} \left( \hat{B}_{t_1, \dots, t_k} - B_{t_1, \dots, t_k} \right) = \frac{1}{\sqrt{n}} \sum_{i=1}^n v_{t_1, \dots, t_k}(\mathcal{D}_i) + \sqrt{n}(\mathbb{P}_n - \mathbb{P})(\hat{v}_{t_1, \dots, t_k}(\mathcal{D}) - v_{t_1, \dots, t_k}(\mathcal{D})) + \sqrt{n}R_2, \tag{29}$$

where  $\hat{v}_{t_1, \dots, t_k}(\mathcal{D}) = (\hat{\varphi}(\mathcal{D}; t_1), \dots, \hat{\varphi}(\mathcal{D}; t_k))^T$ , with  $\hat{\varphi} = \hat{\gamma}^{(1)} - \hat{\gamma}^{(0)} - \hat{\beta}$ . We analyze each component independently. The first term on the right hand side is a sum of mean 0, finite variance random vectors, with the right  $n^{-1/2}$  scaling, and by the Central Limit Theorem this converges to a multivariate normal distribution with mean 0 and covariance matrix equal to  $\Sigma_{t_1, \dots, t_k}$ .

We now provide a bound to the second term, which is an *empirical process*. We need to show that this empirical process, which is a random vector, converges in probability to the

0 vector. By Theorem 2.7 in Van der Vaart (2000), convergence of this random vector to 0 is equivalent to component-wise convergence in probability to 0. We thus want to show that each component of the second term is of order  $o_{\mathbb{P}}(1)$ , as long as the assumption of consistency of the projection of the influence functions holds (Kennedy et al., 2020). Conditional on  $\hat{\mathbb{P}}$ , each component of this empirical process has mean 0. In fact, considering an arbitrary component  $q \in \{1, \dots, k\}$ , we have

$$\begin{aligned} \mathbb{E} \left[ \mathbb{P}_n \left( \hat{v}_{t_1, \dots, t_k}^q(\mathcal{D}) - v_{t_1, \dots, t_k}^q(\mathcal{D}) \right) \mid \hat{\mathbb{P}} \right] &= \mathbb{E} \left[ \hat{v}_{t_1, \dots, t_k}^q(\mathcal{D}) - v_{t_1, \dots, t_k}^q(\mathcal{D}) \mid \hat{\mathbb{P}} \right] \\ &= \mathbb{P} \left[ \hat{v}_{t_1, \dots, t_k}^q(\mathcal{D}) - v_{t_1, \dots, t_k}^q(\mathcal{D}) \right]. \end{aligned} \quad (30)$$

Also, the conditional variance is bounded by

$$\begin{aligned} \mathbb{V} \left[ (\mathbb{P}_n - \mathbb{P}) \left( \hat{v}_{t_1, \dots, t_k}^q(\mathcal{D}) - v_{t_1, \dots, t_k}^q(\mathcal{D}) \right) \mid \hat{\mathbb{P}} \right] &= \mathbb{V} \left[ \mathbb{P}_n \left( \hat{v}_{t_1, \dots, t_k}^q(\mathcal{D}) - v_{t_1, \dots, t_k}^q(\mathcal{D}) \right) \mid \hat{\mathbb{P}} \right] \\ &= \frac{1}{n} \mathbb{V} \left[ \hat{v}_{t_1, \dots, t_k}^q(\mathcal{D}) - v_{t_1, \dots, t_k}^q(\mathcal{D}) \mid \hat{\mathbb{P}} \right] \\ &\leq \frac{1}{n} \mathbb{E} \left[ \left( \hat{v}_{t_1, \dots, t_k}^q(\mathcal{D}) - v_{t_1, \dots, t_k}^q(\mathcal{D}) \right)^2 \right]. \end{aligned} \quad (31)$$

Therefore, by iterated expectation and Chebyshev's inequality, we have

$$\mathbb{P} \left[ \frac{\sqrt{n} \left| (\mathbb{P}_n - \mathbb{P}) \left( \hat{v}_{t_1, \dots, t_k}^q(\mathcal{D}) - v_{t_1, \dots, t_k}^q(\mathcal{D}) \right) \right|}{\mathbb{E} \left[ \left( \hat{v}_{t_1, \dots, t_k}^q(\mathcal{D}) - v_{t_1, \dots, t_k}^q(\mathcal{D}) \right)^2 \right]} \geq t \right] \leq \frac{1}{t^2}. \quad (32)$$

Thus, for any  $\varepsilon > 0$ , there exists a  $t = \varepsilon^{-1/2}$  such that the probability above is controlled by  $\varepsilon$ . This yields the result

$$(\mathbb{P}_n - \mathbb{P}) \left( \hat{v}_{t_1, \dots, t_k}^q(\mathcal{D}) - v_{t_1, \dots, t_k}^q(\mathcal{D}) \right) = O_{\mathbb{P}} \left( \frac{\mathbb{E} \left[ \left( \hat{v}_{t_1, \dots, t_k}^q(\mathcal{D}) - v_{t_1, \dots, t_k}^q(\mathcal{D}) \right)^2 \right]}{\sqrt{n}} \right). \quad (33)$$

In turn, because we assume consistency of the projections of influence functions, this implies the desired result.

Finally, by assumption, each component in the third term, the *remainder* of the expansion, is of order  $o_{\mathbb{P}}(1)$ . Summarizing the previous results, we have

$$\sqrt{n} \left( \hat{B}_{t_1, \dots, t_k} - B_{t_1, \dots, t_k} \right) = \frac{1}{\sqrt{n}} \sum_{i=1}^n v_{t_1, \dots, t_k}(\mathcal{D}_i) + o_{\mathbb{P}}(1), \quad (34)$$

from which the required CLT follows.

By Slutsky theorem, the previous result holds also when  $\hat{\Sigma}_{t_1, \dots, t_k} \xrightarrow{p} \Sigma_{t_1, \dots, t_k}$  replaces  $\Sigma_{t_1, \dots, t_k}$ .

### A.3 Theorem 12

According to Theorem 7.5 in Billingsley (2013), we need to show that:

- The finite-dimensional projections of  $\hat{\beta}_{\text{DR-FOS}}$  converge to normal distributions;

- $\lim_{\delta \rightarrow 0} \limsup_{n \rightarrow \infty} \mathbb{P} \left[ w(\hat{\beta}_{\text{DR-FoS}}; \delta) \geq \varepsilon \right] = 0$ , where  $w(\hat{\beta}_{\text{DR-FoS}}; \delta) = \sup_{|s-t| \leq \delta} |\hat{\beta}_{\text{DR-FoS}}(s) - \hat{\beta}_{\text{DR-FoS}}(t)|$  is the *modulus of continuity*.

The first requirement is satisfied by Lemma 10. Here we focus on the second requirement, which is essentially *tightness*, or *stochastic equicontinuity*.

First, by applying the triangle inequality on the modulus of continuity one obtains:

$$\begin{aligned}
w(\hat{\beta}_{\text{DR-FoS}}; \delta) &= \sup_{|s-t| \leq \delta} |\hat{\beta}_{\text{DR-FoS}}(s) - \hat{\beta}_{\text{DR-FoS}}(t)| \\
&\leq \frac{1}{n} \sum_{i=1}^n \left( 1 + \frac{A_i}{\hat{\pi}^{(1)}(X_i)} \right) \sup_{|s-t| \leq \delta} \left| \hat{\mu}^{(1)}(X_i; s) - \hat{\mu}^{(1)}(X_i; t) \right| \\
&\quad + \frac{1}{n} \sum_{i=1}^n \left( 1 + \frac{1 - A_i}{1 - \hat{\pi}^{(1)}(X_i)} \right) \sup_{|s-t| \leq \delta} \left| \hat{\mu}^{(0)}(X_i; s) - \hat{\mu}^{(0)}(X_i; t) \right| \\
&\quad + \frac{1}{n} \sum_{i=1}^n \frac{A_i - \hat{\pi}^{(1)}(X_i)}{\hat{\pi}^{(1)}(X_i)(1 - \hat{\pi}^{(1)}(X_i))} \sup_{|s-t| \leq \delta} |\mathcal{Y}_i(s) - \mathcal{Y}_i(t)| \\
&= M(\hat{\beta}_{\text{DR-FoS}}; \delta).
\end{aligned} \tag{35}$$

Notice that  $w(\hat{\beta}_{\text{DR-FoS}}; \delta) \geq 0$ . Therefore, by Markov inequality, it holds that:

$$\mathbb{P} \left[ w(\hat{\beta}_{\text{DR-FoS}}; \delta) \geq \varepsilon \right] \leq \frac{\mathbb{E} \left[ w(\hat{\beta}_{\text{DR-FoS}}; \delta) \right]}{\varepsilon} \leq \frac{\mathbb{E} \left[ M(\hat{\beta}_{\text{DR-FoS}}; \delta) \right]}{\varepsilon}, \tag{36}$$

where the second inequality follows from Eq. 35. Crucially, by Assumption 6c and the use of cross-fitting,  $\hat{\pi}^{(1)}(X_i)$  is bounded away from 0 and 1 with probability 1. This ensures the uniform boundedness in probability of the inverse weights,  $(1 + A_i/\hat{\pi}^{(1)}(X_i))$  and  $(1 + (1 - A_i)/(1 - \hat{\pi}^{(1)}(X_i)))$ , which is necessary for the Markov inequality argument to hold. We can now take limits, and obtain:

$$\lim_{\delta \rightarrow 0} \limsup_{n \rightarrow \infty} \mathbb{P} \left[ w(\hat{\beta}_{\text{DR-FoS}}; \delta) \geq \varepsilon \right] \leq \lim_{\delta \rightarrow 0} \limsup_{n \rightarrow \infty} \frac{\mathbb{E} \left[ M(\hat{\beta}_{\text{DR-FoS}}; \delta) \right]}{\varepsilon}. \tag{37}$$

The three terms in  $M(\hat{\beta}_{\text{DR-FoS}}; \delta)$  can all be bounded using the assumptions on expected Hölder continuity. In fact, exploiting the assumption of no unmeasured confounding and assumption 6d, the first term is

$$\limsup_{n \rightarrow \infty} \frac{1}{n} \sum_{i=1}^n \mathbb{E} \left[ 1 + \frac{A_i}{\hat{\pi}^{(1)}(X_i)} \right] \mathbb{E} \left[ \sup_{|s-t| \leq \delta} \left| \hat{\mu}^{(1)}(X_i; s) - \hat{\mu}^{(1)}(X_i; t) \right| \right] \xrightarrow{\delta \rightarrow 0} 0. \tag{38}$$

A similar argument holds for the second term. The third term is

$$\limsup_{n \rightarrow \infty} \frac{1}{n} \sum_{i=1}^n \mathbb{E} \left[ \frac{A_i - \hat{\pi}^{(1)}(X_i)}{\hat{\pi}^{(1)}(X_i)(1 - \hat{\pi}^{(1)}(X_i))} \right] \mathbb{E} \left[ \sup_{|s-t| \leq \delta} |\mathcal{Y}_i(s) - \mathcal{Y}_i(t)| \right] \xrightarrow{\delta \rightarrow 0} 0, \tag{39}$$

where we used assumption 6e.

Finally, the estimator  $\hat{\beta}_{\text{DR-FoS}}$  is defined as a linear combination of continuous functions ( $\mathcal{Y}_i$  and the estimated continuous regression functions  $\hat{\mu}^{(a)}$ ), ensuring that  $\hat{\beta}_{\text{DR-FoS}}$  is a continuous function and therefore a measurable element of  $C(\mathcal{T})$ .

## Appendix B. Functional IPW

Here, we operate in the space  $C(\mathcal{T})$  equipped with the Borel  $\sigma$ -algebra generated by the sup-norm topology. Since the outcome  $\mathcal{Y}$  is continuous, the pointwise operations (multiplication by the scalar weights and difference) preserve continuity, confirming that the map

$$(X, A, \mathcal{Y}) \mapsto \frac{A\mathcal{Y}}{\hat{\pi}^{(1)}(X)} - \frac{(1-A)\mathcal{Y}}{1 - \hat{\pi}^{(1)}(X)} \quad (40)$$

is a measurable element of  $C(\mathcal{T})$ .

The *functional inverse probability weighting* (IPW) estimator is then defined as

$$\hat{\beta}_{\text{IPW}} = \frac{1}{n} \sum_{i=1}^n \left[ \frac{A_i \mathcal{Y}_i}{\hat{\pi}^{(1)}(X_i)} - \frac{(1-A_i) \mathcal{Y}_i}{1 - \hat{\pi}^{(1)}(X_i)} \right]. \quad (41)$$

We first show that the functional IPW is unbiased if the true propensity score is known.

**Proposition 17** *Under Assumptions 1 (identifiability), if  $\hat{\pi}^{(1)} = \pi^{(1)}$  a.s., one has*

$$\mathbb{E} \left[ \hat{\beta}_{\text{IPW}} \right] = \beta. \quad (42)$$

**Proof** By properties of expectation and by the law of iterated expectations, we have

$$\begin{aligned} \mathbb{E} \left[ \hat{\beta}_{\text{IPW}} \right] &= \frac{1}{n} \sum_{i=1}^n \left[ \mathbb{E} \left[ \frac{A\mathcal{Y}}{\hat{\pi}^{(1)}(X)} \right] - \mathbb{E} \left[ \frac{(1-A)\mathcal{Y}}{1 - \hat{\pi}^{(1)}(X)} \right] \right] \\ &= \mathbb{E} \left[ \mathbb{E} \left[ \frac{A\mathcal{Y}}{\hat{\pi}^{(1)}(X)} \mid X \right] \right] - \mathbb{E} \left[ \mathbb{E} \left[ \frac{(1-A)\mathcal{Y}}{1 - \hat{\pi}^{(1)}(X)} \mid X \right] \right] \\ &= \mathbb{E} \left[ \frac{\mathbb{E}[A \mid X]}{\hat{\pi}^{(1)}(X)} \mathbb{E}[\mathcal{Y}^{(1)} \mid X] \right] - \mathbb{E} \left[ \frac{\mathbb{E}[1-A \mid X]}{1 - \hat{\pi}^{(1)}(X)} \mathbb{E}[\mathcal{Y}^{(0)} \mid X] \right] \\ &= \mathbb{E} \left[ \mathcal{Y}^{(1)} - \mathcal{Y}^{(0)} \right] \\ &= \beta. \end{aligned} \quad (43)$$

■

The previous result implies that if  $\hat{\pi}^{(1)} \xrightarrow{P} \pi^{(1)}$ , then the functional IPW will be consistent estimator of the FATE.

We now show that the functional IPW asymptotically behaves as a Gaussian process if the true propensity score is known. First, we introduce the following assumptions.

**Assumption 18 (Inference for IPW)** *Assume that:*

**a.** For any  $t, s \in \mathcal{T}$ ,  $\Sigma(s, t) = \text{cov}(\zeta(t), \zeta(s)) < \infty$ , where  $\zeta(t) = \frac{A\mathcal{Y}(t)}{\hat{\pi}^{(1)}(X)} - \frac{(1-A)\mathcal{Y}(t)}{1 - \hat{\pi}^{(1)}(X)}$ .

**b.** Given  $\xi > 0$ ,  $\pi^{(a)}$  is bounded away from  $\xi$  and  $1 - \xi$  with probability 1.

c. For any  $\delta > 0$ , the functional outcome satisfies

$$\mathbb{E} \left[ \sup_{|s-t| \leq \delta} |\mathcal{Y}(s) - \mathcal{Y}(t)| \right] \leq L\delta^\tau \quad (44)$$

for some constants  $L \geq 0$  and  $\tau > 0$ .

**Theorem 19** Under Assumptions 1 (identifiability) and 18 (inference), if  $\hat{\pi}^{(1)} = \pi^{(1)}$  a.s., one has

$$\sqrt{n} \left( \hat{\beta}_{IPW} - \beta \right) \rightsquigarrow \mathcal{GP}(0, \Sigma), \quad (45)$$

where  $\Sigma(s, t) = \text{cov}(\zeta(t), \zeta(s))$ ,  $\zeta(t) = \frac{A\mathcal{Y}(t)}{\hat{\pi}^{(1)}(X)} - \frac{(1-A)\mathcal{Y}(t)}{1-\hat{\pi}^{(1)}(X)}$ .

**Proof** The proof of this result follows again from Theorem 7.5 in Billingsley (2013). In particular, the standard Central Limit Theorem guarantees that scaled finite-dimensional projections of  $\hat{\beta}_{IPW}$  converge to multivariate normal distributions. It remains to be shown that the condition on the modulus of continuity holds. This follows from the proof of Theorem 12, setting  $\hat{\mu}^{(1)} = \hat{\mu}^{(0)} = 0$ .  $\blacksquare$

**Remark 20** The IPW estimator can alternatively be interpreted as an expectation taken under a weighted law, effectively a change of measure via a Radon-Nikodým derivative between the observational and counterfactual laws (Bruns-Smith et al., 2025; Raykov et al., 2025). Our Gaussian Process limit for  $\hat{\beta}_{IPW}$  (Theorem 19) confirms the expected functional Central Limit Theorem behavior for this weighted empirical process. Under the positivity condition (Assumption 18b), the weights are bounded, and combined with the continuity of sample paths (Assumption 18c), this is sufficient to ensure tightness in  $C(\mathcal{T})$ , aligning our result with the theoretical frameworks developed under the RN perspective.

## Appendix C. Further simulation details

## C.1 Additional simulation results

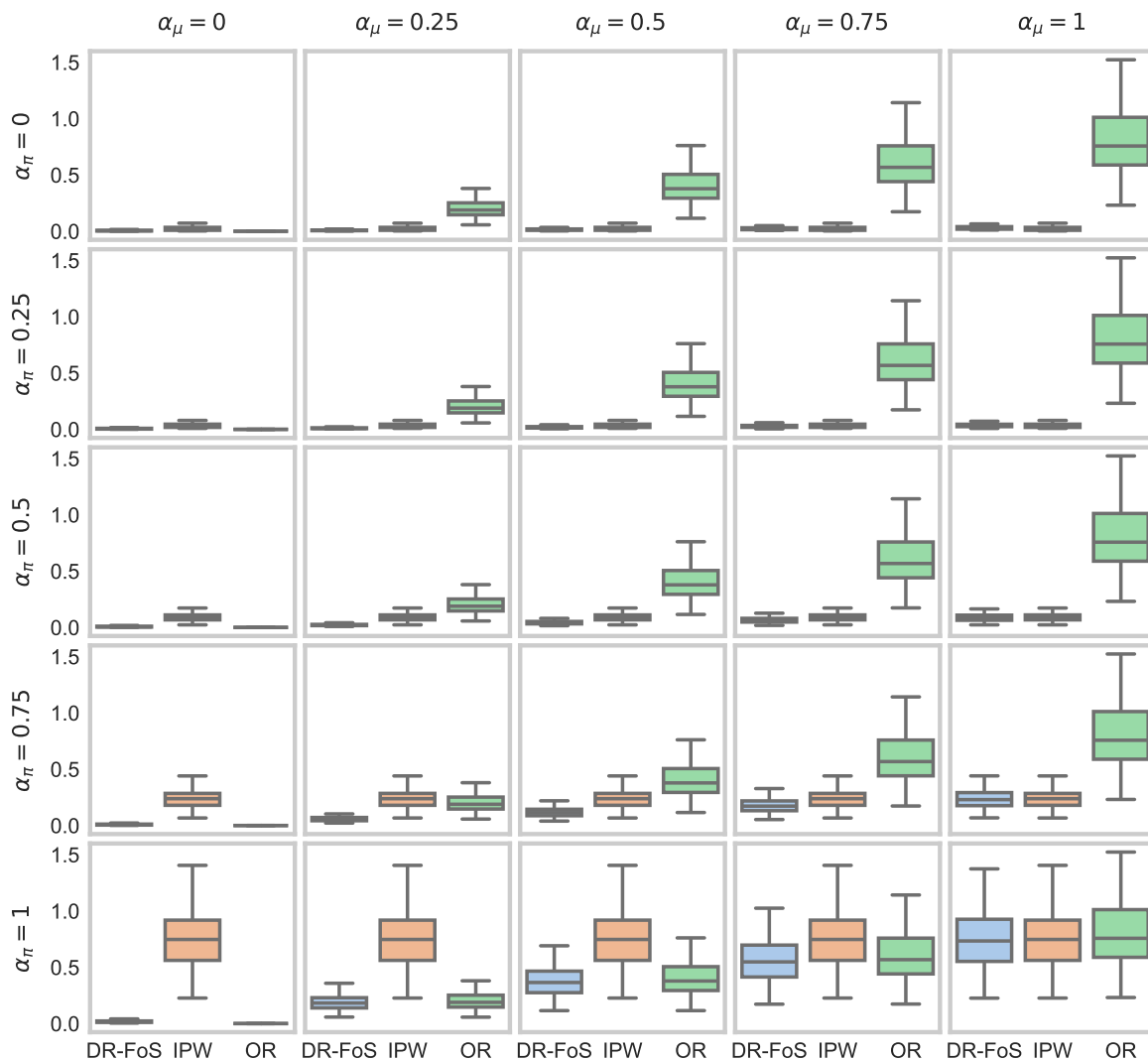


Figure 3: Results of simulation study run as described in Section 4. Each panel displays estimation performance of DR-FoS, IPW and OR under different  $\alpha_\mu$  and  $\alpha_\pi$ . For each box, the center line represents the median; the lower and upper hinges correspond to the first and third quartiles; the upper and lower whiskers span 1.5 times the interquartile range. DR-FoS consistently matches or outperforms the other estimators, demonstrating the strength of double robustness.

## C.2 Simulations with non-smooth trajectories

Here, we repeat the simulation study described in Section 4, adding discontinuities to the regression functions. We expect that, in the presence of sharp local irregularities (as jumps or cusps), simultaneous coverage bands can become overly large. Instead of using smooth regression functions, we generate the true regression functions according to the model

$$\mu^{(a)}(t) = a\tilde{\beta}(t) + \rho(t) + 3\mathbb{1}^{(a)}(t), \quad a \in \{0, 1\}, \quad (46)$$

where the  $\tilde{\beta}$  and the baseline function  $\rho$  are drawn from a 0 mean Gaussian process with a Matern covariance function as before, while  $\mathbb{1}^{(a)}(t)$  is defined as:

$$\mathbb{1}^{(a)}(t) = \begin{cases} 1 & a = 1, 0 \leq t \leq 1/3 \\ 1 & a = 0, 2/3 \leq t \leq 1 \\ 0 & \text{otherwise.} \end{cases} \quad (47)$$

The true FATE in this simulation is  $\beta(t) = \tilde{\beta}(t) + 3\mathbb{1}^{(a)}(t)$ .

Figure 4 confirms our intuition: to maintain valid 95% coverage guarantee under this new setting with discontinuities, DR-FoS enlarges the width of the confidence bands.

## C.3 Simulations with an alternative, explicit formulation

We complement the main simulation study by presenting an additional scenario based on an explicit function-on-scalar data generating process with linear structure, mimicking the setting presented by Liu et al. (2024). This simulation study closely mirrors classical function-on-scalar regression setups and serves to validate the robustness of the proposed estimator DR-FoS against model misspecification.

For each unit  $i = 1, \dots, n$ , we generate covariates  $X_i \in \mathbb{R}^p$ , with  $p = 5$  and  $X_i \sim \text{Unif}(-1, 1)^p$ ; treatment assignments  $A_i \sim \text{Ber}(\pi(X_i))$ , where the propensity score takes the logistic form  $\pi(X_i) = (1 + \exp(-X_i^T \eta + \epsilon_i))^{-1}$ , the coefficients  $\eta \in \mathbb{R}^p$  are drawn once from  $\mathcal{N}(0, I_p)$ , and random noise is sampled according to  $\epsilon_i \sim \mathcal{N}(0, 1)$ ; potential outcomes  $\mathcal{Y}_i^{(0)} = \sum_{j=1}^p X_i \theta_j^{(0)} + \varepsilon_i$  and  $\mathcal{Y}_i^{(1)} = \sum_{j=1}^p X_i \theta_j^{(1)} + D + \varepsilon_i$ , where each  $\theta_j^{(0)}$  and  $\theta_j^{(1)}$  are drawn from a Gaussian process with a Matern covariance function as in Equation 21, with parameters  $l = 0.25$ ,  $\nu = 3.5$ , and choose  $\eta = 1$ ,  $D$  is a constant function set at 1, and the functional error  $\varepsilon_i$  is drawn pointwise from a standard normal distribution; the observed outcome is  $\mathcal{Y}_i = A_i \mathcal{Y}_i^{(1)} + (1 - A_i) \mathcal{Y}_i^{(0)}$ ; the true functional average treatment effect (FATE) is  $\beta = \mathbb{E} [\mathcal{Y}_i^{(1)} - \mathcal{Y}_i^{(0)}]$ .

We estimate  $\beta$  using the outcome regression model in Equation 26, the IPW estimator in Equation 27, and DR-FoS as defined in Equation 6. All estimators employ a logistic regression model for learning  $\hat{\pi}^{(a)}$ , while we exploit both standard function-on-scalar linear models (Kokoszka and Reimherr, 2017) and a state-of-the-art machine learning method, called FunGCN (Boschi et al., 2024b), to learn  $\hat{\mu}^{(a)}$ . To fit FunGCN, we set the following hyperparameters: *forecast\_ratio* = 0, *pruning* = 0.7, *k\_gcn* = 10, *lr* =  $5e - 5$ , *max\_selected* = 5, *k\_graph* = 3, *nhid* = [32, 32], *epochs* = 50, *batch\_size* = 1, *dropout* = 0, *kernel\_size* = 0, *patience* = 5, *min\_delta* = 0, *val\_size* = 0, *test\_size* = 0. We refer to Boschi et al. (2024b) for an in-depth description of these hyperparameters.

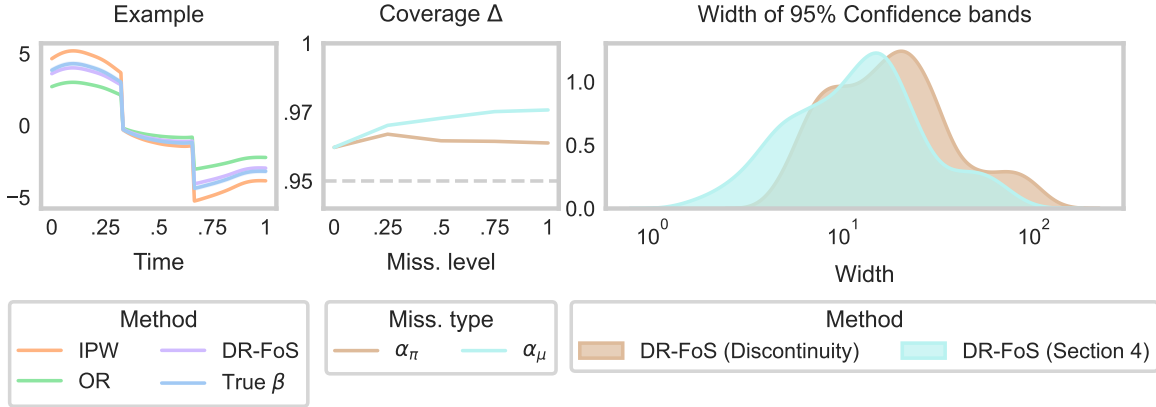


Figure 4: Simulation results based on the data generating process described in Section 4 with the discontinuity in the regression functions as described in Appendix Section C.2. The first panel (leftmost) shows an example of true FATE  $\beta$  (blue) as generated by our simulation scheme, and the estimates provided by IPW (orange), OR (green) and DR-FoS (purple). In this example we set  $\alpha_\mu = 0.25$  and  $\alpha_\pi = 0.75$ . The second panel shows the average coverage levels achieved under misspecifications of the regression functions (light blue,  $\alpha_\pi = 0$ ) and of the propensity score (brown,  $\alpha_\mu = 0$ ). The grey dashed line represents the nominal 95% coverage level. The third panel (rightmost) compares the average widths of the 95% simultaneous confidence bands from two simulations, displayed on a logarithmic axis. Specifically, it plots the distribution of the average band width from the simulation with regression function discontinuities against the average band width from the original (continuous) simulation (described in Section 4). The plot clearly demonstrates that the introduction of discontinuities poses a significant challenge. To maintain the 95% coverage guarantee under these conditions, DR-FoS robustly manages the issue by enlarging the width of the confidence band.

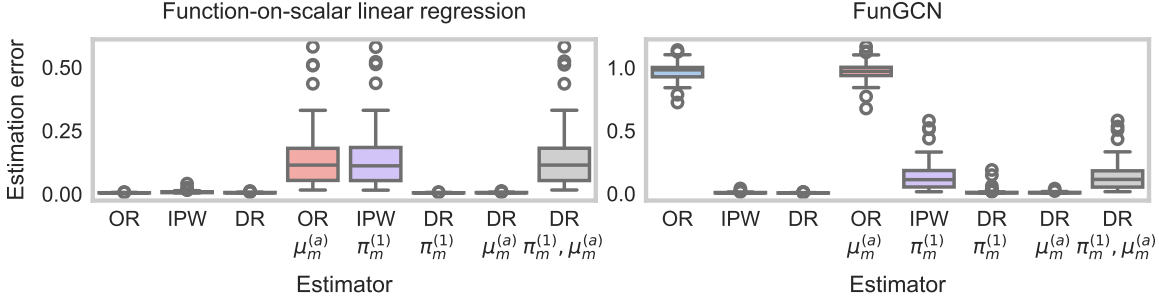


Figure 5: Results of the simulation study described in Appendix Section C.3. Each panel shows the estimation performance of DR-FoS, IPW, and OR under both well-specified and misspecified settings. Misspecification is introduced by fitting nuisance functions using transformed covariates  $\tilde{X}_i$ ,  $i = 1, \dots, n$ . Misspecified outcome regressions are denoted by  $\mu_m^{(a)}$ , and misspecified propensity scores by  $\pi_m^{(1)}$ . For example, OR  $\mu_m^{(a)}$  refers to the outcome regression estimator fitted with a misspecified regression function, DR  $\pi_m^{(1)}$  denotes the DR-FoS estimator fitted with a misspecified propensity score but well-specified regression functions, while DR  $\pi_m^{(1)}, \mu_m^{(a)}$  denotes the DR-FoS estimator constructed using both a misspecified propensity score and misspecified regression functions. For each box, the center line represents the median; the lower and upper hinges correspond to the first and third quartiles; the upper and lower whiskers span 1.5 times the interquartile range. DR-FoS consistently matches or outperforms the other estimators, demonstrating the strength of double robustness.

To assess robustness, we introduce a misspecified feature set  $\tilde{X}_i \in \mathbb{R}^3$ , derived from the original covariates via nonlinear and interaction terms:

$$\tilde{X}_i = \begin{bmatrix} \sin(X_{i1}) \\ (X_{i2} + X_{i3})^2 \\ \log(1 + |X_{i4}|) \end{bmatrix}. \quad (48)$$

Under well-specified scenarios, both the outcome regression and propensity score models are fitted using  $X_i$ . Under misspecification, nuisance models are fitted using  $\tilde{X}_i$  instead of  $X_i$ . All other aspects of the simulation, including the true data-generating process, remain unchanged.

We repeat each experiment across 50 independent random seeds. The results are summarized in Figure 5. Under well-specified conditions, the outcome regression (OR) estimator based on a linear function-on-scalar model exhibits excellent performance, with consistently low estimation error across replications. In contrast, the OR estimator using FunGCN displays slightly higher variability due to the model’s tendency to oversmooth functional predictions. The IPW estimator also performs strongly in the well-specified setting, and as predicted by theory, DR-FoS matches or exceeds this performance by combining both nuisance components. In particular, when FunGCN is used for outcome regression, DR-FoS clearly benefits from the IPW correction, compensating for the oversmoothing bias. In misspecified scenar-

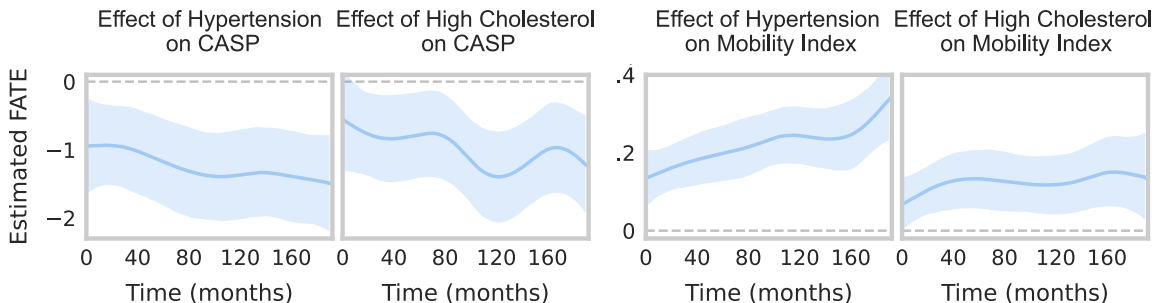


Figure 6: SHARE application results using FunGCN as model for the regression function. Each panel displays a different estimated causal effect. Blue continuous lines correspond to DR-FoS estimates; blue bands are 95% asymptotic simultaneous confidence bands obtained by repeatedly sampling from the Gaussian process; grey dotted horizontal lines correspond to 0.

ios, both the OR and IPW estimators degrade significantly, confirming their sensitivity to model misspecification. In contrast, DR-FoS maintains superior performance when either the regression or the propensity score model is correctly specified, and provides comparable performance even when both are misspecified. Notably, in the FunGCN setting, DR-FoS consistently outperforms the misspecified OR estimator, once again highlighting the value of the IPW correction in mitigating outcome model bias.

## Appendix D. Additional real-data analysis

In addition to the analysis presented in the main text, here we provide a further robustness check, where we use a state-of-the-art machine learning method for functional data called FunGCN (Boschi et al., 2024b), to fit the regression model  $\hat{\mu}^{(a)}$ . FunGCN, which leverages a Graph Convolutional Network architecture, serves as a non-linear function-on-scalar regression tool. It is specifically designed to handle multimodal data and learn complex dependencies between functional outcomes and scalar/vector covariates, even on irregular observation grids. This approach differs from earlier work like funcNN (Thind et al., 2020) by explicitly using graph-based message passing to capture dependencies across the functional domain and integrate scalar covariates efficiently into the network. To fit FunGCN, we set the following hyperparameters: *forecast\_ratio* = 0, *pruning* = 0.7, *k\_gcn* = 10, *lr* =  $5e - 5$ , *max\_selected* = 5, *k\_graph* = 3, *nhid* = [32, 32], *epochs* = 50, *batch\_size* = 1, *dropout* = 0, *kernel\_size* = 0, *patience* = 5, *min\_delta* = 0, *val\_size* = 0, *test\_size* = 0. We refer to Boschi et al. (2024b) for an in-depth description of these hyperparameters.

The estimation strategy is the same as in the main text. For each combination of chronic disease and functional outcome, we fit DR-FoS using FunGCN for the regression function  $\hat{\mu}^{(a)}$ , and logistic regression for the propensity score  $\hat{\pi}^{(a)}$ . We employ cross-fitting with 5 balanced folds. Results are shown in Figure 6 and fully align with the findings in the main text, supporting their robustness.